Cell Metabolism
Article

CaMKII-Mediated Phosphorylation of the Myosin Motor Myo1c Is Required for Insulin-Stimulated GLUT4 Translocation in Adipocytes

Ming Fai Yip,[1] Georg Ramm,[1] Mark Larance,[1,2] Kyle L. Hoehn,[1] Mark C. Wagner,[3] Michael Guilhaus,[2] and David E. James[1,*]
[1]Diabetes and Obesity Research Program, Garvan Institute of Medical Research, Darlinghurst, NSW 2010, Australia
[2]Bioanalytical Mass Spectrometry Facility, University of New South Wales, Sydney, NSW 2052, Australia
[3]Department of Medicine, Indiana University School of Medicine, Indianapolis, IN 46202, USA
*Correspondence: d.james@garvan.org.au
DOI 10.1016/j.cmet.2008.09.011

SUMMARY

The unconventional myosin Myo1c has been implicated in insulin-regulated GLUT4 translocation to the plasma membrane in adipocytes. We show that Myo1c undergoes insulin-dependent phosphorylation at S701. Phosphorylation was accompanied by enhanced 14-3-3 binding and reduced calmodulin binding. Recombinant CaMKII phosphorylated Myo1c in vitro and siRNA knockdown of CaMKIIδ abolished insulin-dependent Myo1c phosphorylation in vivo. CaMKII activity was increased upon insulin treatment and the CaMKII inhibitors CN21 and KN-62 or the Ca^{2+} chelator BAPTA-AM blocked insulin-dependent Myo1c phosphorylation and insulin-stimulated glucose transport in adipocytes. Myo1c ATPase activity was increased after CaMKII phosphorylation in vitro and after insulin stimulation of CHO/IR/IRS-1 cells. Expression of wild-type Myo1c, but not S701A or ATPase dead mutant K111A, rescued the inhibition of GLUT4 translocation by siRNA-mediated Myo1c knockdown. These data suggest that insulin regulates Myo1c function via CaMKII-dependent phosphorylation, and these events play a role in insulin-regulated GLUT4 trafficking in adipocytes likely involving Myo1c motor activity.

INTRODUCTION

Insulin increases glucose uptake into muscle and fat cells by triggering the translocation of the facilitative glucose transporter GLUT4 from intracellular storage vesicles (GSVs) to the plasma membrane (PM). This involves multiple steps, each of which invokes the activity of numerous proteins. For example, the biogenesis of GSVs involves coat proteins and other factors (Millar et al., 1999); the storage of these vesicles reportedly involves sequestration factors (Yu et al., 2007); the movement of GSVs to the cell periphery involves motor proteins and microtubules (Olson et al., 2001; Tong et al., 2001); once at the cell periphery the GSVs specifically interact with the plasma membrane in a multistage process involving tethering factors such as the exocyst followed by SNARE-mediated docking and fusion (Inoue et al., 2003; Kanzaki and Pessin, 2001; Martin et al., 1998; Yang et al., 2001).

Recent progress in defining key insulin-regulated steps has been derived from two separate approaches: the use of a membrane fusion assay in which some aspects of the process have been reconstituted in vitro (Koumanov et al., 2005), and the use of total internal reflection fluorescence microscope (TIRFM), a high-resolution method for studying events close to the PM in living cells (Bai et al., 2007; Huang et al., 2007). Both of these methods indicate that the PM is a major regulatory node for insulin action. In particular, the latter method dissected the encounter of GSVs with the PM into multiple steps and showed that a step downstream of vesicle docking is the major insulin-regulated step (Bai et al., 2007). This has provided important information in the search for key molecules that function at the intersection point between signaling and vesicle transport.

The PI3K/Akt pathway plays a central role in regulating glucose transport in muscle and fat cells, and so identifying downstream targets of Akt, particularly those acting at the PM, is an important goal. One such target is the RabGAP TBC1D4/AS160, the phosphorylation of which plays an essential yet incomplete role in GLUT4 trafficking (Sano et al., 2003). Overexpression of a TBC1D4 mutant, in which each of the Akt phosphorylation sites have been mutated, in adipocytes blocks insulin-stimulated GLUT4 translocation (Sano et al., 2003). However, using TIRFM it has been shown that the function of TBC1D4 is most closely linked to GSV docking, which as described above seems to be a relatively minor insulin-regulated step (Bai et al., 2007).

One approach to identify phosphoproteins that are activated in response to a variety of cellular triggers is to use phosphoprotein binding domains as affinity matrices as an enrichment step in combination with mass spectrometry. One such binding intermediate that has been particularly useful in identifying phosphoproteins, associated with tyrosine kinase signaling pathways is the 14-3-3 family of proteins (Yaffe et al., 1997). The overlap in the consensus sites for 14-3-3 protein binding and a number of AGC kinase family members is very high. 14-3-3 binding has been exploited previously to identify phosphoproteins from HeLa cells (Meek et al., 2004; Rubio et al., 2004) and HEK293 cells (Benzinger et al., 2005; Jin et al., 2004).

We describe here the use of this approach for the identification of a novel insulin-regulated phosphoprotein in adipocytes, the

unconventional motor protein Myo1c. This is a particularly exciting observation because Myo1c acts principally at the PM, playing an important role in a diverse set of physiological processes including the translocation of ion channels within the membranes of stereocilia in vestibular hair cells of the ear (Batters et al., 2004; Phillips et al., 2006; Stauffer et al., 2005), cytoskeletal rearrangement and membrane protrusion in neuronal growth cones (Wang et al., 2003), and antidiuretic hormone-regulated delivery of sodium channels to the brush border of kidney epithelial cells (Wagner et al., 2005). Myo1c is also involved in the insulin-regulated delivery of GLUT4 to the PM in adipocytes (Bose et al., 2002, 2004). Reduced expression of Myo1c in adipocytes using siRNA or overexpression of the Myo1c tail domain, as a dominant inhibitor, both impair insulin stimulated translocation of GLUT4 to the PM (Bose et al., 2002; Huang et al., 2005).

RESULTS

Identification of Myo1c as a 14-3-3-Interacting Protein

Many downstream targets of insulin, including TBC1D4, GSK3, and BAD, bind to 14-3-3 upon phosphorylation. To identify insulin-regulated phosphoproteins in insulin-sensitive cell types we undertook a comprehensive proteomic analysis of insulin-regulated 14-3-3-interacting proteins in insulin-sensitive tissues. 14-3-3-interacting proteins were isolated from whole cell lysates of insulin-treated cells using a 14-3-3β affinity matrix. Interacting proteins were resolved by SDS-PAGE followed by mass spectrometry analysis (Figure 1A). Using this strategy we identified >400 putative 14-3-3-binding proteins from insulin-stimulated cells (Table S1), 75% of which contain at least one 14-3-3 mode 1 consensus site (RSXpS/TXP) according to the Scansite program with greater than medium stringency. A number of known insulin-regulated phosphoproteins including 6-phosphofructo-2-kinase, Bcl2-antagonist of cell death (BAD), Forkhead in rhabdomyosarcoma (FKHR), glycogen synthase kinase-3 (GSK-3), insulin receptor substrate 1 (IRS1), PI3K regulatory domain p85, tuberous sclerosis 1 and 2 (TSC1-TSC2), and TBC1D4 (Mackintosh, 2004; Wilker and Yaffe, 2004) were identified confirming the validity of our 14-3-3 purification approach.

One of the most interesting proteins identified in this screen was the unconventional myosin Myo1c. The sequence coverage of Myo1c (Swiss-Prot accession number: MYO1C_MOUSE, Q9WTI7) purified from the PM was 37.2% compared to only 3.6% from the cytosol, suggesting that the PM is the major location where 14-3-3 interacts with Myo1c. This interaction was not observed in rat muscle tissue, suggesting that this interaction may be specific to adipocytes. To confirm this interaction endogenous Myo1c was immunoprecipitated from 3T3-L1 adipocytes. Sypro Ruby staining revealed bands of molecular weight 120 kDa and 30 kDa (data not shown). Mass spectrometry analysis of these bands revealed that they corresponded to Myo1c and several 14-3-3 isoforms, respectively. This suggests that there is little 14-3-3 isoform specificity in this interaction.

Insulin Regulates Myo1c Phosphorylation and 14-3-3 Binding

The unconventional myosin motor protein Myo1c fulfilled many of our designated criteria. Myo1c is known to play a role in GLUT4 trafficking in adipocytes (Bose et al., 2002, 2004), and it was enriched in the PM fraction (Table S1). The in vitro interaction of Myo1c with 14-3-3 was confirmed by immunoblotting using a Myo1c specific monoclonal antibody (Figure 1B). Insulin increased the amount of Myo1c associated with 14-3-3 compared to that observed under basal conditions, and this effect was abolished by the PI3K inhibitor Wortmannin. Similar data were obtained when EYFP-tagged Myo1c, and GST-tagged 14-3-3β were coexpressed in CHO/IR/IRS-1 cells, indicating that the insulin-dependent association of Myo1c and 14-3-3 occurs in vivo (Figure 1C). One possible explanation for the insulin-dependent interaction between Myo1c and 14-3-3 is that Myo1c may interact with another protein that is phosphorylated in response to insulin. To exclude this possibility, we performed a GST-overlay assay using GST-14-3-3 (Figure 1D). EYFP-Myo1c was immunoprecipitated from CHO/IR/IRS-1 cells, subjected to SDS-PAGE, and transferred to PVDF membrane and incubated with GST-14-3-3. There was a direct association between 14-3-3 and Myo1c using this approach, and we observed increased binding of 14-3-3 to Myo1c isolated from insulin-treated cells compared to non-insulin-treated cells. To prove that this interaction was due to Myo1c phosphorylation, the PVDF membrane was incubated with alkaline phosphatase prior to the overlay, and this completely abolished the interaction. These findings demonstrate that insulin stimulates Myo1c phosphorylation in adipocytes, resulting in its interaction with 14-3-3 proteins.

Myo1c Is Phosphorylated on S701 in Response to Insulin

Analysis of the Myo1c primary amino acid sequence by either Scansite and Phospho-MAP identified multiple potential phosphorylation and 14-3-3-binding sites. Site-directed mutagenesis was used to map putative phosphorylation sites in Myo1c. Residues S142, T564, and S701 were initially chosen for site directed mutagenesis. S142 has a high stringency mode 2 consensus 14-3-3-binding motif (RXXXpS/TXP), T564 and S701 were identified as potential mode 1 consensus 14-3-3-binding motifs (RSXpS/TXP); and T564 is also a potential Akt phosphorylation motif. Each of these sites was mutated to Ala, and mutants were expressed in CHO/IR/IRS-1 cells. As shown in Figure 1E, Myo1c WT and the S142A and T564A mutants interacted to a similar extent with 14-3-3 in an insulin-regulated manner. However, mutation of S701 completely inhibited the 14-3-3/Myo1c interaction. Based on these data, we conclude that S701 is the major insulin-regulated phosphorylation site in Myo1c that regulates 14-3-3 binding.

The Role of Myo1c Phosphorylation in Calmodulin Binding

It is of interest that S701 is located at the start of the Myo1c neck domain proximal to the four calmodulin-binding IQ motifs (Figure 2A). Increased calcium displaces calmodulin from one or more of these IQ domains (Gillespie and Cyr, 2002), and so we reasoned that phosphorylation may play a role in calmodulin binding. Phosphorylation at S701 may either affect calmodulin binding to IQ1 or calmodulin binding may regulate Myo1c phosphorylation at S701. To test these possibilities, we generated an IQ1A mutant, in which four of the five residues of the IQ consensus sequence of IQ1 were mutated to Ala (Figure 2A). This mutation was previously shown to prevent calmodulin binding

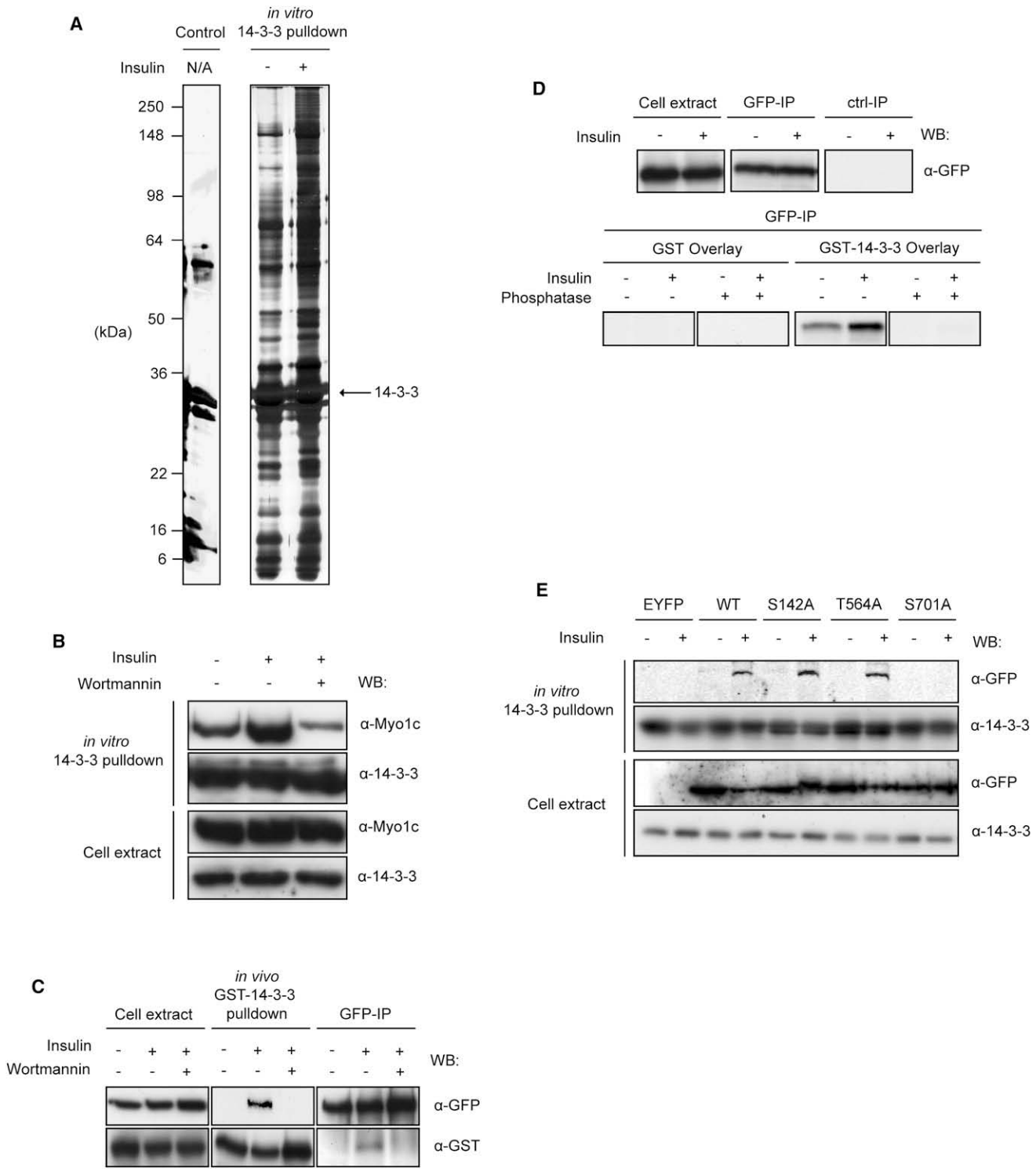

Figure 1. Identification of Myo1c as an Insulin-Regulated Phosphoprotein

(A) 14-3-3-pulldown from 3T3-L1 adipocytes. 3T3-L1 adipocytes were stimulated with 100 nM insulin for 30 min, and lysates were incubated with 14-3-3 sepharose beads overnight; beads were washed and bound proteins eluted with SDS-PAGE sample buffer followed by separation of the proteins by SDS-PAGE. 14-3-3 sepharose without incubation with lysate was used as control. To detect total protein, the gel was silver stained.

(B) In vitro association of 14-3-3 and Myo1c in 3T3-L1 adipocytes. Cell lysate from either basal, insulin-treated, or Wortmannin/insulin-treated (100 nM Wortmannin for 10 min prior to insulin stimulation) 3T3-L1 adipocytes was subjected to 14-3-3 pulldown. Input cell extracts and pulldowns were analyzed by western blot with the use of anti-Myo1c and anti-14-3-3 antibodies. The experiment was performed three times, and the images are from a representative experiment.

to the IQ domain (Phillips et al., 2006). A significant interaction was observed between calmodulin and Myo1c WT in nonstimulated cells, whereas this interaction was reduced by 45% following insulin stimulation ($p < 0.05$ versus basal; Figure 2B). Mutation of the IQ1 domain resulted in a ~31% reduction in calmodulin binding to Myo1c ($p < 0.05$ versus WT/basal) compared to WT Myo1c. The fact that calmodulin binding was not completely ablated in the IQ1 mutant suggests that this domain is not required for calmodulin binding to the adjacent IQ domains. Whereas calmodulin binding to WT Myo1c was reduced with insulin, this was not observed for the S701A and IQ1A mutants (Figure 2B). This suggests that Myo1c S701 phosphorylation and calmodulin binding to IQ1 are mutually exclusive events, raising the question of whether phosphorylation regulates calmodulin binding or vice versa. If calmodulin binding to IQ1 is required for Myo1c phosphorylation, then the IQ1A mutant should display reduced insulin-stimulated phosphorylation and 14-3-3 binding. However, dissociation of calmodulin from IQ1 neither inhibited nor stimulated phosphorylation at S701 (Figure 2C). In contrast, insulin did not stimulate 14-3-3 binding to the double mutant S701AIQ1A, which contains both the phosphorylation site mutation and the IQ1 mutation. These results suggest that calmodulin binding to IQ1 is not required for phosphorylation at S701. Although insulin may also regulate calmodulin binding to other IQ domains, these data suggest that insulin inhibits calmodulin binding to the first IQ domain in Myo1c via phosphorylation at S701.

Calcium/Calmodulin-Dependent Protein Kinase II (CaMKII) Phosphorylates Myo1c

We next sought to identify the Myo1c kinase. In silico analysis revealed S701 is a potential phosphorylation site for PKA, PKC, and CaMKII. As shown in Figure 3A, the PKCζ pseudosubstrate and the Akt inhibitor had no significant effect on insulin-stimulated 14-3-3 binding to Myo1c. In contrast, Wortmannin and KN-62 caused a substantial reduction in the amount of 14-3-3 coimmunoprecipitated with Myo1c from insulin-treated 3T3-L1 adipocytes (Figure 3B). To confirm the role of CaMKII in Myo1c phosphorylation, we utilized a highly specific cell-penetrating CaMKII inhibitor tat-CN21 (Vest et al., 2007). The insulin-stimulated interaction between 14-3-3 and Myo1c was significantly inhibited by tat-CN21, whereas the control peptide, tat-ctrl, was without effect (Figure 3C). To confirm the status of endogenous Myo1c phosphorylation, 3T3-L1 adipocytes were labeled to equilibrium with [^{32}P]orthophosphate, and Myo1c was immunoprecipitated following incubation of cells with or without kinase inhibitors and insulin. Insulin increased the amount of phosphorylated Myo1c in adipocytes in a Wortmannin and tat-CN21-sensitive manner (Figure 3D), consistent with the in vitro 14-3-3 pulldown data.

CaMKII is activated in vivo by increased cytosolic calcium, which triggers calmodulin binding to CaMKII. KN-62 prevents the activation of CaMKII by inhibiting calmodulin binding (Tokumitsu et al., 1990). Intriguingly, chelation of cytosolic calcium with BAPTA-AM inhibits insulin-stimulated glucose transport and GLUT4 translocation in adipocytes (Whitehead et al., 2001). Hence, we next set out to establish if BAPTA-AM inhibits insulin-stimulated Myo1c phosphorylation and 14-3-3 binding. BAPTA-AM almost completely inhibited insulin-stimulated Myo1c phosphorylation as indicated by impaired binding to 14-3-3 (Figure 3E). Conversely, the Ca^{2+} ionophore A23187 increased 14-3-3 binding to Myo1c to a similar extent as insulin (Figure 3F). To further investigate the role of CaMKII in phosphorylation of Myo1c, we utilized an siRNA construct targeting CaMKIIδ, a major isoform expressed in 3T3-L1 adipocytes (Figure 3G). Reduction of CaMKIIδ protein expression by ~90% percent resulted in a significant reduction in insulin-stimulated Myo1c binding to 14-3-3, whereas in cells transfected with a control siRNA we observed an ~2.5-fold increase in Myo1c binding to 14-3-3 with insulin. Based on these results, we propose that CaMKII mediates the insulin-stimulated phosphorylation of Myo1c at S701.

Next, we performed an in vitro phosphorylation assay using recombinant CaMKII and endogenous Myo1c immunoprecipitated from 3T3-L1 adipocytes. An insulin-dependent and KN-62-sensitive Myo1c/14-3-3 interaction was observed in the absence of recombinant CaMKII (Figure 3H). Incubation with active CaMKII, but not inactive CaMKII, enhanced Myo1c/14-3-3-binding under all conditions. Moreover, CaMKII phosphorylation of Myo1c in vitro was sensitive to the CaMKII inhibitor tat-CN21, but not to the control peptide tat-ctrl (Figure 3I).

To confirm that CaMKII phosphorylates Myo1c directly on S701, EYFP-Myo1c WT and the S701A mutant were immunoprecipitated from CHO/IR/IRS-1 cells and incubated with recombinant CaMKII in the presence of [γ^{32}P]ATP. Phosphorylation of Myo1c WT but not the Myo1c S701A mutant was observed with CaMKII (Figure 3J). Hence, we conclude that CaMKII phosphorylates Myo1c both in vitro and in vivo at S701, and

(C) In vivo association of 14-3-3 and Myo1c in CHO/IR/IRS-1 cells. CHO/IR/IRS-1 cells were transiently cotransfected with EYFP-Myo1c and GST-14-3-3β. Cell lysate from either basal, insulin-treated, or Wortmannin/insulin-treated (100 nM Wortmannin for 10 min prior to insulin stimulation) CHO/IR/IRS-1 cells were subjected to pulldown with glutathione sepharose or immunoprecipitation with anti-GFP antibody. Input cell extracts, pulldowns, and immunoprecipitates were analyzed by western blot with the use of anti-GFP and anti-GST antibodies to detect EYFP-Myo1c and GST-14-3-3β, respectively. The experiment was performed three times and the images are from a representative experiment.

(D) Direct and phosphorylation-dependent association of 14-3-3 and Myo1c. CHO/IR/IRS-1 cells were transiently transfected with EYFP-Myo1c. Cell lysate from either basal or insulin-treated cells was subjected to immunoprecipitation with anti-GFP and IgG antibodies. Input cell extracts and immunoprecipitates were analyzed by western blotting with the use of anti-GFP antibody (upper panel). The PVDF membrane containing immunoprecipitated Myo1c was incubated with or without alkaline phosphatase in phosphatase buffer overnight at 37°C. The membrane was probed for binding to either GST or GST-14-3-3 with the use of anti-GST antibody (lower panel). The experiment was performed three times, and the images are from a representative experiment.

(E) Mapping Myo1c phosphorylation sites. CHO/IR/IRS-1 cells were transiently transfected with either EYFP (empty vector), EYFP-Myo1c WT, S142A, T564A, or S701A. Cell lysates from either basal or insulin-treated cells were subjected to 14-3-3 pulldown. Input cell extracts and pulldowns were analyzed by western blot with the use of anti-GFP antibody, which detects EYFP-Myo1c, and anti-14-3-3 antibody. The experiment was performed three times, and the images are from a representative experiment.

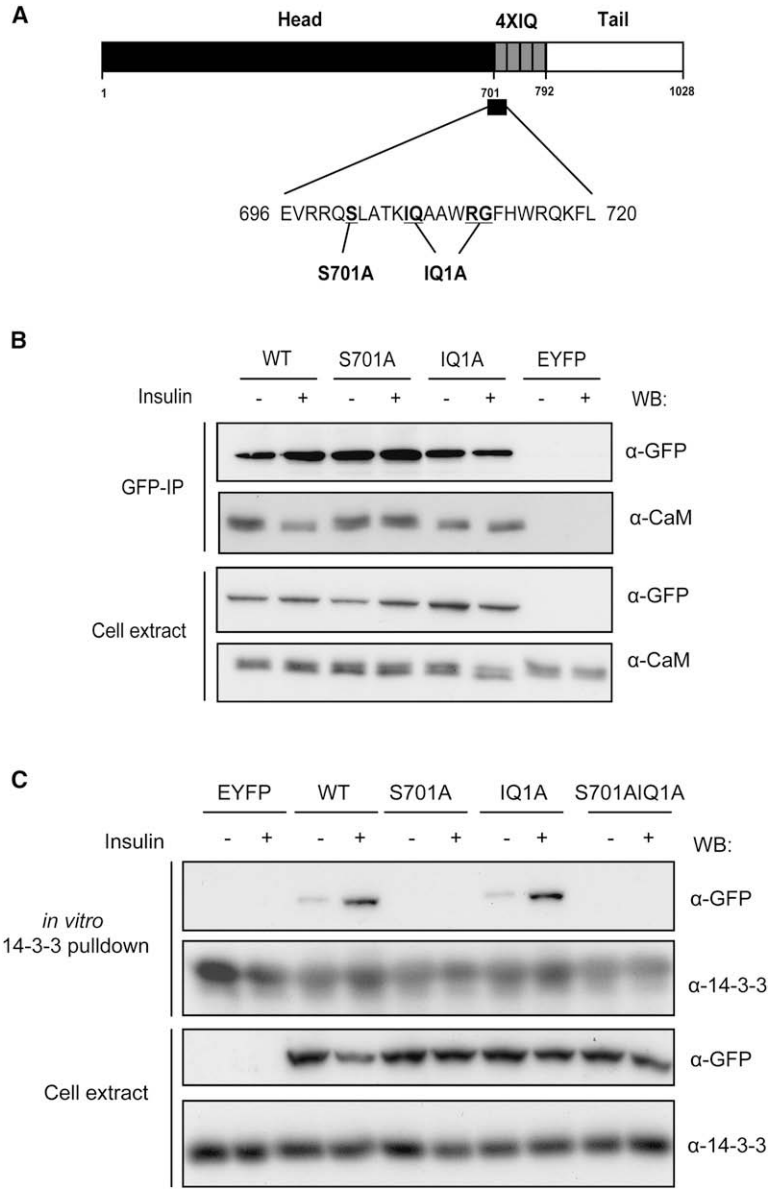

Figure 2. Phosphorylation of Myo1c on S701 Regulates Calmodulin Binding

(A) Domain structure of Myo1c. Myo1c consists of three domains including head, neck, and tail domain. S701A, IQ1A, and S701AIQ1A double mutants were generated in this study. S701A contains a single amino acid change at S701, while IQ1A contains four amino acid mutations (I706A, Q707A, R711A, and G712A).

(B) In vivo association of different Myo1c mutants and calmodulin in CHO/IR/IRS-1 cells. CHO/IR/IRS-1 cells were transiently transfected with either EYFP-Myo1c WT, S701A, IQ1A, or EYFP (empty vector). Cell lysates from either basal or insulin-treated cells were subjected to immunoprecipitation with anti-GFP antibody. Input cell extracts and pulldowns were analyzed by western blot with the use of anti-GFP antibody, which detects EYFP-Myo1c, and anti-CaM antibody. The experiment was performed three times, and the images are from a representative experiment.

(C) In vitro association of different Myo1c mutants and 14-3-3 in CHO/IR/IRS-1 cells. CHO/IR/IRS-1 cells were transiently transfected with either EYFP (empty vector), EYFP-Myo1c WT, S701A, IQ1A, or S701AIQ1A double mutant. Cell lysates from either basal or insulin-treated cells was subjected to 14-3-3 pulldown. Input cell extracts and pulldowns were analyzed by western blot with the use of anti-GFP antibody, which detects EYFP-Myo1c, and anti-14-3-3 antibody. The experiment was performed three times, and the images are from a representative experiment.

that the upstream regulation of CaMKII relies upon Ca^{2+}/CaM-dependent pathways.

To determine if CaMKII activity may regulate the insulin-dependent dissociation of calmodulin and Myo1c as shown earlier (Figure 2B), we pretreated adipocytes with KN62 or tat-CN21. Both compounds, as well as Wortmannin, inhibited the insulin-dependent reduction of calmodulin binding to Myo1c (Figure 3K).

Insulin Induces CaMKII Phosphorylation and Activation in Adipocytes

CaMKII is activated following autophosphorylation at T286 (Colbran et al., 1988). We next sought to determine if insulin activates CaMKII in adipocytes using an anti-pT286 CaMKII antibody. Phosphorylated CaMKII was detected in unstimulated cells, and insulin increased CaMKII phosphorylation in a dose- and time-dependent manner (Figures 4A and 4B). We also observed increased CaMKII kinase activity following incubation of adipocytes with insulin (Figure 4C). These data indicate that CaMKII is activated by insulin in 3T3-L1 adipocytes. Moreover, KN-62 and tat-CN21 inhibited insulin-stimulated glucose transport by 63% and 46%, respectively (Figure 4D), consistent with an important role for this kinase in insulin action.

CaMKII-Dependent Phosphorylation Increases Myo1c ATPase Activity

As the myosin motor family is responsible for actin-based motility, we next examined the role of phosphorylation on Myo1c ATPase activity. Endogenous Myo1c was immunoprecipitated from basal adipocytes and incubated with recombinant CaMKII. CaMKII was removed and Myo1c-bound sepharose was extensively washed with reaction buffer. [γ^{32}P]ATP hydrolysis was assayed in the presence of tat-CN21 to abolish the activity of any remaining CaMKII. An equivalent amount of Myo1c was present in all conditions (Figure 5A). CaMKII, but not inactive CaMKII, stimulated Myo1c ATPase activity by 3- to 4-fold (Figures 5A and 5B). Inclusion of GST-14-3-3 in this assay had no further effect on Myo1c ATPase activity. We next explored if insulin stimulation affects Myo1c ATPase activity in vivo by measuring the ATPase activity of EYFP-Myo1c WT immunoprecipitated from transiently transfected CHO/IR/IRS-1 cells with or without insulin stimulation. Insulin increased the ATPase activity of Myo1c WT by 2-fold (Figures 5C and 5D), whereas a Myo1c ATPase mutant (EYFP-Myo1c K111A), only showed background hydrolysis of ATP,

though it was phosphorylated in response to insulin (data not shown). These data suggest that insulin-stimulated phosphorylation of Myo1c regulates its motor activity and 14-3-3 binding does not appear to play a significant role in this effect at least in vitro.

CaMKII-Dependent Phosphorylation of Myo1c Regulates GLUT4 Translocation

We next set out to establish if Myo1c phosphorylation plays a role in GLUT4 translocation using a knockin approach. An siRNA construct was designed to target the untranslated region of Myo1c mRNA. Expression of this siRNA in adipocytes resulted in a substantial reduction in endogenous Myo1c levels (~85%) (Figure 6A). In agreement with previous studies (Bose et al., 2002), siRNA-mediated reduction in Myo1c in adipocytes significantly reduced insulin-stimulated GLUT4 translocation in 3T3-L1 adipocytes (Figure 6B). Re-expression of WT Myo1c in cells expressing the Myo1c siRNA rescued the block in GLUT4 translocation (Figures 6C and 6D). Strikingly, re-expression of the Myo1c S701A mutant was unable to rescue the defect in insulin-stimulated GLUT4 translocation observed in cells expressing the Myo1c siRNA. These data indicate that Myo1c phosphorylation at S701 plays an essential role in insulin-stimulated GLUT4 translocation in vivo.

As described above, insulin-dependent Myo1c phosphorylation/14-3-3-binding triggers release of calmodulin from the first and possibly additional IQ domains in Myo1c. Hence, this raises the question of whether phosphorylation of Myo1c per se plays an essential role in insulin action or if the major effect is mediated via calmodulin release. To explore this relationship in more detail, we first examined the consequences of reintroducing the Myo1c calmodulin-binding mutant into adipocytes lacking endogenous Myo1c (Figure 6C). Intriguingly, upon insulin stimulation of cells expressing the IQ1A mutant insulin-stimulated GLUT4 translocation was partially restored. However, since calmodulin is not displaced from the Myo1c S701A mutant in response to insulin (Figure 2B), this is consistent with a possible role for both phosphorylation/14-3-3 binding and calmodulin release in the function of Myo1c in insulin-mediated GLUT4 translocation. To further elucidate the importance of both steps, we used the S701AIQ1A double mutant. If phosphorylation/14-3-3 binding simply regulates Myo1c function via displacement of calmodulin, then the S701AIQ1A mutant should phenocopy the IQ1A mutant. Intriguingly, that was not the case pointing toward a role of phosphorylation/14-3-3 independent of calmodulin displacement as the important insulin-regulated step. Notably, expression of the IQ1A mutant in adipocytes resulted in a significant increase in non-insulin-dependent GLUT4 translocation (Figure 6D). As shown in Figure 2C, this mutant does not display increased phosphorylation under basal conditions, suggesting that regulated calmodulin binding to Myo1c per se may play an additional role in this process. Hence, these data suggest that both calmodulin binding in the basal state and phosphorylation after insulin-stimulation may regulate the function of Myo1c in GLUT4 translocation.

To explore the relationship between Myo1c ATPase activity and GLUT4 translocation in adipocytes, we reintroduced the ATPase catalytic domain mutant in Myo1c knockdown adipocytes. Re-expression of Myo1c K111A was unable to rescue the defect in insulin-stimulated GLUT4 translocation mediated by knockdown of Myo1c (Figures 6C and 6D). This suggests that Myo1c ATPase activity is required for insulin-stimulated GLUT4 translocation in adipocytes.

DISCUSSION

In the present study we show that the myosin motor Myo1c undergoes increased phosphorylation in response to insulin. In view of the important role of Myo1c in GLUT4 trafficking (Bose et al., 2002), this represents a key advance in this area. Insulin stimulates Myo1c phosphorylation at a site that flanks one of its major calmodulin-binding domains. Insulin-dependent Myo1c phosphorylation is regulated by CaMKII in a PI3K-dependent manner resulting in reduced calmodulin binding to Myo1c and concomitant association with 14-3-3 proteins. The observation that the Myo1c IQ1A mutant undergoes normal insulin-dependent phosphorylation suggests that calmodulin binding to the first IQ domain is not required for Myo1c phosphorylation, excluding the possibility that this domain is required for CaMKII binding. Further studies are required to determine if the additional IQ domains are required for CaMKII-dependent Myo1c phosphorylation. Notwithstanding, our data suggest a role for Myo1c phosphorylation in calmodulin release. Phosphorylation has been shown to play an important role in calmodulin binding to other IQ domain proteins. Serine phosphorylation of neuromodulin at a variable residue within its consensus IQ domain (IQxpSxRGxxxR) regulates calmodulin binding (Chapman et al., 1991). A crystal structure of the IQ domains from MyoV and apo-Calmodulin reveals a role for acidic residues in calmodulin in this interaction (Houdusse et al., 2006). Hence, the introduction of an additional negative charge in this vicinity as in phosphorylated Myo1c would likely impair this interaction (pSxxxxIQxxxRGxxxR). Alternatively, binding of 14-3-3 upon phosphorylation could lead to steric displacement of calmodulin.

How could Myo1c phosphorylation and/or regulated calmodulin binding play a role in the function of this molecule? It has been reported that calmodulin binding to Myo1c inhibits its actin-stimulated ATPase activity and Myo1c ATPase activity is stimulated by calcium (Barylko et al., 1992; Chacko et al., 1994; Zhu et al., 1996, 1998). In the present study we show that CaMKII-mediated phosphorylation stimulates Myo1c ATPase activity. Hence, this leads to a model where insulin may regulate the mechanical properties of Myo1c via Ca^{2+}/CaMKII-dependent phosphorylation. To formally test this hypothesis it will be necessary to precisely identify the consequences of Ca^{2+} loading and phosphorylation on Myo1c function in vivo. It is also conceivable that insulin-dependent Myo1c phosphorylation and 14-3-3 binding may regulate the association of other proteins, such as cargo, since 14-3-3 possesses at least two phosphopeptide binding sites.

Another possibility is that phosphorylation may regulate the association of Myo1c with the PM. Myo1c and Myo1c orthologs bind to anionic phospholipids (Barylko et al., 2005) via a PIP_2 binding site located in the Myo1c tail domain (Hokanson et al., 2006; Reizes et al., 1994). Consistent with a potential role for calmodulin binding in the membrane association of Myo1c, Tang and colleagues (Tang et al., 2002) showed that Ca^{2+} regulates the binding affinity of Myo1c to lipids. This poses a potential

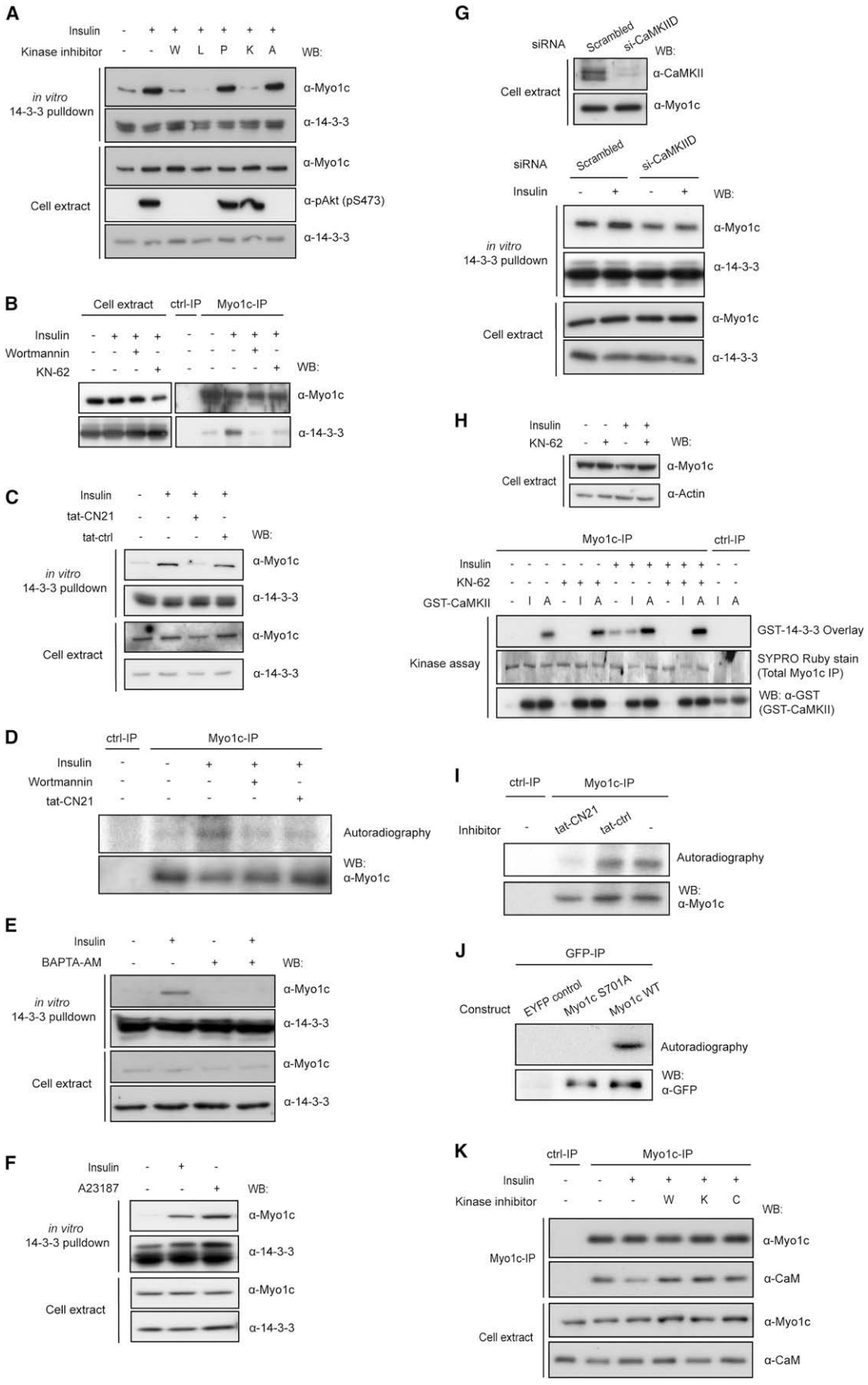
A
Insulin
Kinase inhibitor
W L P K A
WB:
in vitro
14-3-3 pulldown
α-Myo1c
α-14-3-3
Cell extract
α-pAkt (pS473)
B
Cell extract
ctrl-IP
Myo1c-IP
Wortmannin
KN-62
C
tat-CN21
tat-ctrl
D
Autoradiography
E
BAPTA-AM
F
A23187
G
siRNA
Scrambled
si-CaMKIID
α-CaMKII
H
α-Actin
I
Inhibitor
J
GFP-IP
Construct
EYFP control
Myo1c S701A
Myo1c WT
α-GFP
K
Kinase inhibitor
α-CaM

model where Myo1c phosphorylation at S701 may stabilize membrane association of Myo1c. Intriguingly, we did not observe a significant reduction in insulin-stimulated CaMKII phosphorylation in adipocytes at T286 using the PI3K inhibitor Wortmannin, suggesting that activation of CaMKII by insulin is PI3K independent. However, insulin-stimulated phosphorylation of Myo1c was PI3K dependent. This raises the possibility that PI3K may regulate the accessibility of Myo1c to CaMKII in vivo either by regulating membrane association of Myo1c or CaMKII itself. Noteably, CaMKII phosphorylation is regulated via dynamic subcellular localization of both substrate and kinase (Tsui et al., 2005). Further studies are required to resolve these aspects of Myo1c regulation by Ca^{2+}, CaMKII, and PI3K.

Another intriguing element of the present study is the role of CaMKII and Ca^{2+} in insulin-regulated glucose transport. Although controversial, inhibition of this process using Ca^{2+} chelators (Whitehead et al., 2001) and CaMKII inhibitors has been described (Brozinick et al., 1999; Konstantopoulos et al., 2007) consistent with our data (Figure 4D). The use of inhibitors of ill-defined specificity, such as KN-62, the inability to document insulin-dependent changes in cytosolic Ca^{2+} and CaMKII activity, and the lack of insulin-regulated CaMKII substrates in adipocytes have provided major obstacles in substantiating the role of Ca^{2+} in insulin action. In the present study we have overcome several of these obstacles by showing that a highly specific CaMKII inhibitor tat-CN21 inhibits insulin stimulated glucose

Figure 3. CaMKII Phosphorylates Myo1c on S701

(A) Effect of different kinase inhibitors on in vitro 14-3-3 binding of Myo1c. 3T3-L1 adipocytes were pretreated with either 100 nM Wortmannin (W) for 10 min, 50 μM LY294002 (L) for 30 min, 5 μM PKCζ pseudosubstrate (P) for 1 hr, 10 μM KN-62 (K) for 45 min, or 5 μM Akt inhibitor (A) for 30 min prior to insulin stimulation. Cell lysate from either basal, insulin-treated, or kinase inhibitors/insulin-treated 3T3-L1 adipocytes was subjected to 14-3-3 pulldown. Input cell extracts and pulldowns were analyzed by western blot with the use of anti-Myo1c, anti-14-3-3, and anti-pAkt (pS473) antibodies. The experiment was performed three times, and the images are from a representative experiment.

(B) Effect of Wortmannin and KN-62 on in vivo 14-3-3 binding of Myo1c. 3T3-L1 adipocytes were pretreated with either 100 nM Wortmannin for 10 min or 10 μM KN-62 for 45 min for 30 min prior to insulin stimulation. Cell lysate from either basal, insulin-treated, or kinase inhibitors/insulin-treated 3T3-L1 adipocytes was subjected to immunoprecipiration using anti-Myo1c antibody and irrelevant antibodies (ctrl-IP). Input cell extracts and immunoprecipitates were analyzed by western blot with the use of anti-Myo1c and anti-14-3-3 antibodies. The experiment was performed three times, and the images are from a representative experiment.

(C) Effect of CaM-KIIN-derived peptides, tat-CN21, on in vitro 14-3-3 binding of Myo1c. 3T3-L1 adipocytes were pretreated with either 5 μM tat-CN21 or control peptide (tat-ctrl) for 30 min prior to insulin stimulation. Cell lysate from either basal, insulin-treated, or inhibitor/insulin-treated 3T3-L1 adipocytes was subjected to 14-3-3 pulldown. Input cell extracts and pulldowns were analyzed by western blot with the use of anti-Myo1c and anti-14-3-3 antibodies. The experiment was performed three times, and the images are from a representative experiment.

(D) In vivo ^{32}P labeling of Myo1c in 3T3-L1 adipocytes. 3T3-L1 adipocytes were labeled with [^{32}P]orthophosphate. Cells were incubated with insulin or kinase inhibitors as indicated. Cell lysates were subjected to immunoprecipitation with anti-Myo1c and irrelevant antibodies (ctrl-IP). Immunoprecipitates were analyzed by autoradiography and immunoblotting with the use of anti-Myo1c antibody. The experiment was performed two times, and the images are from a representative experiment.

(E) Effect of Ca^{2+} chelator, BAPTA-AM, on in vitro 14-3-3-binding of Myo1c. 3T3-L1 adipocytes were pretreated with 50 μM BAPTA-AM for 30 min prior to insulin stimulation. Cell lysate from either basal, insulin-treated, or BAPTA-AM/insulin-treated 3T3-L1 adipocytes was subjected to 14-3-3 pulldown. Input cell extracts and pulldowns were analyzed by western blot with the use of anti-Myo1c and anti-14-3-3 antibodies. The experiment was performed three times, and the images are from a representative experiment.

(F) Effect of Ca^{2+} ionophore, A23187, on in vitro 14-3-3 binding of Myo1c under basal condition. 3T3-L1 adipocytes were treated with 5 μM A23187 for 15 min. Cell lysate from either basal, insulin-treated, or A23187-treated 3T3-L1 adipocytes was subjected to 14-3-3 pulldown. Input cell extracts and pulldowns were analyzed by western blot with the use of anti-Myo1c and anti-14-3-3 antibodies. The experiment was performed three times, and the images are from a representative experiment.

(G) Effect of siRNA-mediated CaMKII knockdown on in vitro 14-3-3 binding of Myo1c. 3T3-L1 adipocytes were electroporated with either scrambled or CaMKIIδ-targeted siRNA. After 48 hr, cell lysate from either basal or insulin-treated cells was subjected to 14-3-3 pulldown. Input cell extracts and pulldowns were analyzed by western blot with the use of anti-CaMKII, anti-Myo1c and anti-14-3-3 antibodies. The experiment was performed three times, and the images are from a representative experiment.

(H) In vitro CaMKII phosphorylation assay of Myo1c. 3T3-L1 adipocytes were either untreated, treated with KN-62 (10 μM for 1 hr) only, insulin only, or pretreated with KN-62 (10 μM for 45 min) prior to insulin stimulation. Cell lysates were subjected to immunoprecipitation with anti-Myo1c antibody. Input cell extracts were analyzed by western blot with the use of anti-Myo1c and anti-Actin antibodies (upper panel). The immunocomplex-bound protein G sepharose was incubated with kinase assay buffer containing either no GST-CaMKII, inactive GST-CaMKII (I), or active GST-CaMKII (A). The kinase reactions were stopped by boiling in sample buffer, resolved by SDS-PAGE, and transferred to PVDF membrane. The amounts of GST-CaMKII were detected by western blot with anti-GST antibody. To detect the amounts of Myo1c immunoprecipitated in each condition, the PVDF membrane containing immunoprecipitated Myo1c was stained with SYPRO Ruby protein blot stain. The membrane was then probed for binding to GST-14-3-3 with the use of anti-GST antibody to detect the in vitro 14-3-3 binding of immunoprecipitated Myo1c (lower panel). The experiment was performed three times, and the images are from a representative experiment.

(I) Effect of tat-CN21 on in vitro CaMKII phosphorylation assay of Myo1c. Cell lysate from basal 3T3-L1 adipocytes were subjected to immunoprecipitation with anti-Myo1c antibody and were subjected to in vitro CaMKII phosphorylation as described in Figure 3H in the presence of [$\gamma^{32}P$]ATP and either 1 μM tat-CN21 or 1 μM tat-ctrl. Immunoprecipitates were analyzed by autoradiography and Western blot with the use of anti-Myo1c antibody. The experiment was performed two times and the images are from a representative experiment.

(J) In vitro CaMKII phosphorylation assay of Myo1c WT and S701A. CHO/IR/IRS-1 cells were transiently transfected with either EYFP (empty vector), EYFP-Myo1c S701A, or EYFP-Myo1c WT. Cell lysate from basal CHO/IR/IRS-1 cells were subjected to immunoprecipitation with anti-GFP antibody and were subjected to in vitro CaMKII phosphorylation as described in Figure 3H in the presence of [$\gamma^{32}P$]ATP. Immunoprecipitates were analyzed by autoradiography and western blot with the use of anti-GFP antibody. The experiment was performed two times, and the images are from a representative experiment.

(K) Effect of different kinase inhibitors on in vivo calmodulin binding of Myo1c. 3T3-L1 adipocytes were pretreated with either 100 nM Wortmannin (W) for 10 min, 10 μM KN-62 (K) for 45 min, or 5 μM tat-CN21 (C) for 30 min prior to insulin stimulation. Cell lysates were subjected to immunoprecipitation using anti-Myo1c antibody. Input cell extracts and immunoprecipitates were analyzed by western blot with the use of anti-Myo1c and anti-calmodulin antibodies. The experiment was performed three times, and the images are from a representative experiment.

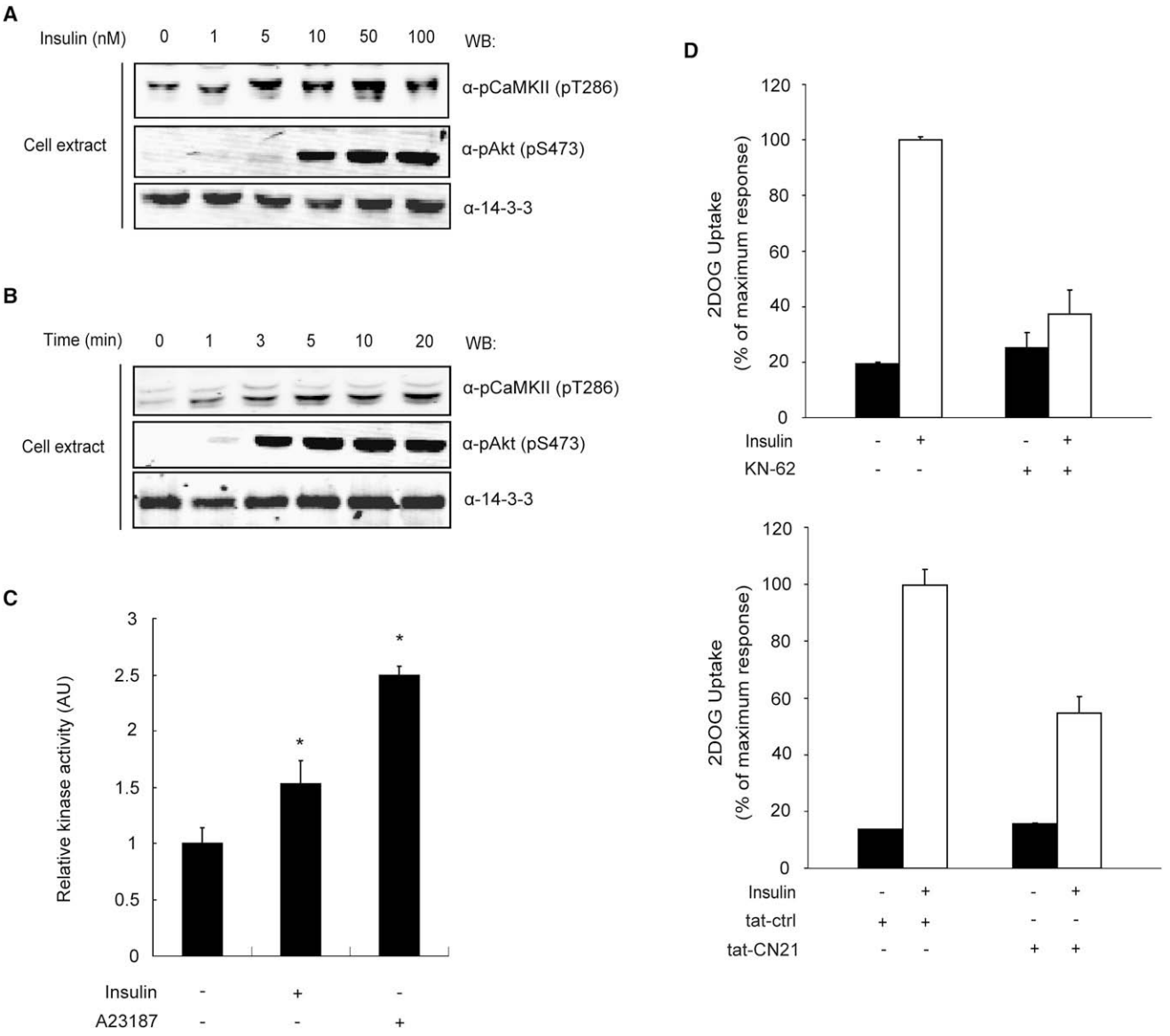

Figure 4. Insulin Stimulates CaMKII Activation in 3T3-L1 Adipocytes

(A) Dose response of insulin signaling. 3T3-L1 adipocytes were serum-starved and stimulated with insulin at the indicated concentrations for 20 min. The cell extracts were analyzed by western blot with the use of anti-pCaMKII (T286), anti-pAkt (pS473), and anti-14-3-3 antibodies. The experiment was performed three times, and the images are from a representative experiment.

(B) Time course of insulin signaling. 3T3-L1 adipocytes were serum-starved and stimulated with 100 nM insulin for 1 to 20 min as indicated. The cell extracts were analyzed by western blot with the use of anti-pCaMKII (T286), anti-pAkt (pS473), and anti-14-3-3 antibodies. The experiment was performed three times, and the images are from a representative experiment.

(C) In vitro CaMKII kinase activity assay. 3T3-L1 adipocytes were either untreated, treated with insulin, or treated with 5 μM A23187 for 20 min. Cell lysates were subjected to immunoprecipitation with anti-CaMKII antibody, and the kinase activity assay was preformed directly on the agarose beads by measuring the ^{32}P labeling of the peptide substrate. The ratio of autonomous activity to maximal activity was calculated for each condition, and the ratio corresponding to the unstimulated cells was normalized to 1 arbitrary unit. The value of each condition represents the mean ± SEM of three independent experiments. *$p < 0.05$ versus basal condition.

(D) Effect of CaMKII inhibitors on insulin-stimulated [^{3}H]-2-deoxyglucose (2DOG) uptake in 3T3-L1 adipocytes. 3T3-L1 adipocytes were either treated with DMSO (basal) only, insulin (100 nM for 15 min) only, KN-62 (10 μM for 1 hr) only, or pretreated with KN-62 (10 μM for 45 min) prior to insulin stimulation (upper panel). In another experiment, 3T3-L1 adipocytes were either treated with tat-ctrl (5 μM for 45 min) only, tat-CN21 (5 μM for 45 min) only, or pretreated with either of the peptides (5 μM for 30 min) prior to insulin stimulation (lower panel). The average 2DOG uptake of each condition is shown as percentage of maximum response of insulin-treated cells and represents the mean ± SEM of three independent experiments, in which each experiment was assayed in triplicate.

transport in adipocytes (Figure 4D); insulin activates CaMKII in adipocytes consistent with a recent study in rat muscle (Wright et al., 2004); and Myo1c as an important insulin-regulated CaMKII substrate in the fat cell. Notably, we have been unable to observe Myo1c phosphorylation in muscle, raising the possibility that an alternate myosin isoform may substitute for Myo1c in this cell type. While we have not directly examined the effects of insulin on intracellular Ca^{2+} in the adipocyte, a previous study has shown that insulin increases the Ca^{2+} concentration just beneath the PM in isolated skeletal muscle (Bruton et al., 1999). This raises the possibility that the insulin effect on Ca^{2+} homeostasis may be highly localized in these cells. This may be relevant to the effect of insulin on CaMKII activity, Myo1c phosphorylation, and the insulin-dependent release of calmodulin from Myo1c, all of which likely occur just beneath the PM. Intriguingly, CaMKII is activated at specific subcellular locations in other cell types (Davies et al., 2007; Inagaki et al., 2000), which may explain why there is only a modest increase in CaMKII kinase activity induced by insulin when analyzed in vitro. This also provides challenges in dissecting some of these steps in vivo. This is particularly evident for the effects of insulin on the Myo1c/calmodulin interaction, which may require the development of highly sensitive FRET-based methods to ensure that the changes in calmodulin binding that we have observed (Figure 2B) are not due to changes after cell lysis. Regardless, the effect of insulin on Myo1c/calmodulin interaction as a minimum likely reflects reduced affinity between Myo1c and calmodulin in vivo, thus underpinning a role for S701 phosphorylation in causing a conformational change in Myo1c at or around IQ1. Furthermore, the observation that the IQ1A mutant caused a slight increase in cell surface GLUT4 levels when expressed in Myo1c-knockdown adipocytes is consistent with a role for regulated calmodulin binding at this site.

The present study poses a number of key questions. What is the role of Myo1c in the insulin-regulated encounter of GLUT4 vesicles with the PM? TIRFM studies indicate that a major insulin-regulated step occurs proximal to the docking of vesicles with the cell surface (Bai et al., 2007). Could Myo1c be the major regulator of this step, and if so how? Currently we can only speculate on this action of Myo1c, but it is intriguing that in the case of other myosin motors an intimate relationship between myosin function and SNARE assembly has been shown. For example, MyoVa directly associates with the t-SNARE Syntaxin1a (Watanabe et al., 2005). Hence, it will be of interest to determine how Myo1c function intersects with SNARE assembly in the adipocyte and as to whether such functions are mediated via phosphorylation, calmodulin release, or 14-3-3 binding. It will also be of interest to explore the effect of insulin on cell-surface Ca^{2+} channels in the adipocyte. Finally, clarifying the role of PI3K in the insulin-dependent regulation of Ca^{2+} homeostasis, CaMKII activation, and Myo1c phosphorylation will be essential in order to determine the relationship of this pathway to the Akt pathway.

In conclusion, Myo1c represents a novel target of insulin action in adipocytes, and we propose the following model as a framework for future studies. In the basal state, calmodulin binds to the IQ1 domain of Myo1c. Upon insulin stimulation, Ca^{2+} influx increases the concentration of Ca^{2+} just beneath the PM, activating CaMKII, Myo1c phosphorylation at S701, and 14-3-3 binding to Myo1c. Phosphorylation and/or 14-3-3 binding leads to displacement of calmodulin from the Myo1c IQ1 domain. A key functional outcome of this pathway is increased Myo1c ATPase activity. This likely plays a key role in GLUT4 vesicle docking and/or fusion at the plasma membrane, either by regulating the movement of vesicles along cortical actin filaments or by stabilizing the association of the vesicles and possibly other proteins close to the PM, thus increasing their likelihood of fusion.

EXPERIMENTAL PROCEDURES

Plasmids, Antibodies, and Inhibitors

The pEYFP-Myo1c plasmid was a gift from Michael Czech (University of Massachusetts Medical School; Worcester, MA) and was used to generate pEYFP-Myo1c S142A, T564A, S701A, IQ1A (I706A, Q707A, R711A, and G712A), S701AIQ1A, and K111A using the QuikChange II XL Site-Directed Mutagenesis Kit from Stratagene (La Jolla, CA). The pBabe-HA-GLUT4, pGEX-14-3-3β plasmid and the mammalian expressing GST-14-3-3β plasmid was previously described (Ramm et al., 2006). Recombinant 14-3-3β expressed as a glutathione-*S*-transferase (GST) fusion protein in *E. coli* was purified by standard procedures using Glutathione-4B sepharose (GE Healthcare; Uppsala, Sweden). The GST tag of the recombinant GST-14-3-3β protein was removed by Thrombin protease before coupling to CNBr-activated sepharose (GE Healthcare). For immunoblotting and immunoprecipitation of Myo1c, previously characterized antibody was used (Wagner et al., 1992). Anti-14-3-3β, anti-Actin, and anti-CaMKII antibodies were from Santa Cruz (Santa Cruz, CA). Anti-calmodulin antibody was from Upstate (Lake Placid, NY). Anti-pAkt (pS473) was from Cell Signaling Technology (Beverly, MA). Anti-pCaMKII (pT286) antibody was from Promega (Madison, WI). Anti-GST antibody was from GE Healthcare. Anti-HA antibody was from Covance Research Products (Richmond, CA). Anti-GFP antibody for immunoprecipitation and western blot was from Roche (Indianapolis, IN), and anti-GFP antibody for immunoflorescence was from Molecular Probes (Leiden, the Netherlands). Secondary antibodies for western blot were purchased from GE Healthcare. Alexa Fluor 488- and Cy3-conjugated secondary antibodies for immunoflorescence staining were from Molecular Probes and Jackson ImmunoResearch (West Grove, PA). Akt inhibitor (Akti-1/2) was obtained from Peter Shepherd (University of Auckland, New Zealand) and previously described (DeFeo-Jones et al., 2005). CaMKII inhibitor peptide tat-CN21 and tat-ctrl were obtained from Ulrich Bayer (University of Colorado Denver; Aurora, CO) and previously described (Vest et al., 2007). A23187, Wortmannin, PKCζ pseudosubstrate, and KN-62 were from Sigma (Sydney, Australia). LY294002 and BAPTA-AM were purchased from Calbiochem (San Diego, CA).

SiRNA, Cell Culture, Cell Treatments, and Transfection

The scrambled siRNA (target sequence, 5′-CAGUCGCGUUUGCGACUGG-3′), Myo1c-targeted siRNA (si-Myo1c, target sequence, 5′-AAGCUUCCAGA CAGGGAUCCAUG-3′), and CaMKIIδ-targeted siRNA (si-CaMKIID, target sequence, 5′-GGAGUCAACUGAGAGCUCA-3′) were purchased from Dharmacon (Lafayette, CO) and previously described (Bose et al., 2002; Ishiguro et al., 2006). 3T3-L1 fibroblasts were cultured and differentiated into adipocytes as described (Larance et al., 2005). 3T3-L1 fibroblasts were infected with pBABE-HA-GLUT4 retrovirus as previously described (Ramm et al., 2006). Differentiated 3T3-L1 adipocytes were transfected by electroporation as described (Bose et al., 2002). For transfection of siRNA, 20 nmol of siRNA was used per 10 cm dish. For cotransfection of plasmids and si-Myo1c, 100 μg of DNA and 20 nmol of siRNA were used per 10 cm dish. CHO/IR/IRS-1 cells were cultured and transiently transfected using Lipofectamine 2000 (Invitrogen, Carlsbad, CA) as described earlier (Ramm et al., 2006).

Pulldown, Immunoprecipitation, and 14-3-3 Overlay Assay

Transfected CHO/IR/IRS-1 cells, or 3T3-L1 adipocytes were incubated in serum-free Dulbecco's modified Eagle's medium (Invitrogen) for 2 hr, stimulated with 100 nM insulin (Calbiochem) for 15 min or preincubated with kinase inhibitors prior to insulin stimulation, and lysed in lysis buffer (1% Nonidet P-40,

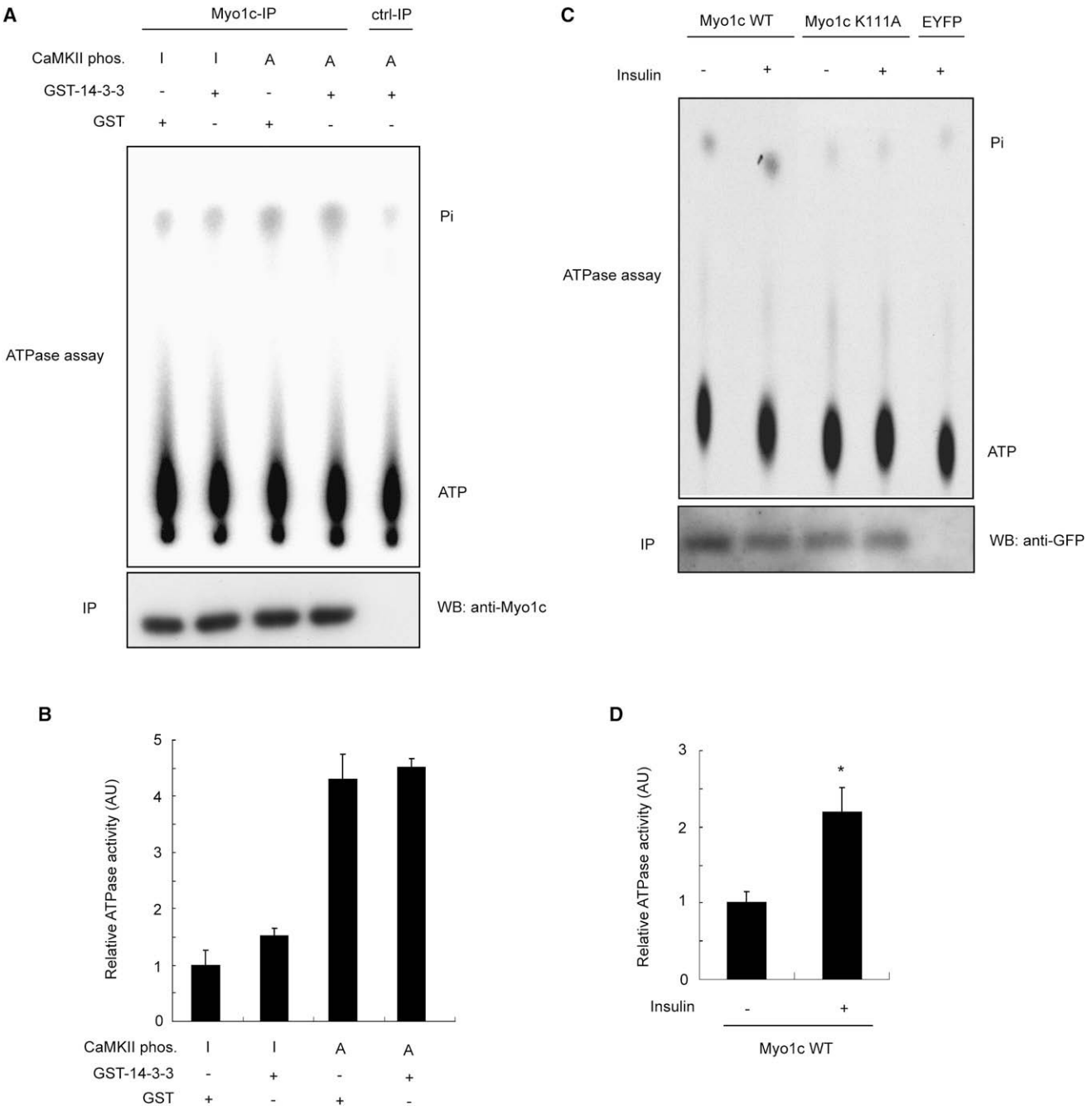

Figure 5. Phosphorylation of Myo1c Increases In Vitro ATPase Activity

(A) Effect of in vitro CaMKII phosphorylation and 14-3-3 binding on ATPase activity of Myo1c. Basal 3T3-L1 adipocyte lysates were subjected to immunoprecipitation with anti-Myo1c antibody and irrelevant antibody (ctrl). The immunocomplex-bound protein G sepharose was incubated with either inactive GST-CaMKII (I) or active GST-CaMKII (A), followed by either 46 ng GST or 100 ng GST-14-3-3 for 30 min at room temperature. GST-CaMKII and any unbound GST-14-3-3 were removed by washing of the beads with ATPase reaction buffer. The precipitates were incubated with [γ^{32}P]ATP, and reactions were subjected to thin-layer chromatography. Hydrolyzed [γ^{32}P]Pi and unhydrolyzed [γ^{32}P]ATP are indicated on the right. Immunoprecipitates were analyzed by western blot with the use of anti-Myo1c antibody. The experiment was performed three times, and the images are from a representative experiment.

(B) Quantification of ATPase assays. The values of [γ^{32}P]Pi and [γ^{32}P]ATP were measured by densitometry. The ratio of [γ^{32}P]Pi to [γ^{32}P]ATP was calculated, and the control signal (ctrl-IP) was subtracted. The ratio corresponding to the precipitate incubated with inactive GST-CaMKII and GST was normalized to 1 arbitrary unit. The value of each condition represents the mean ± SEM of three independent experiments.

(C) Effect of insulin stimulation on ATPase activity of EYFP-Myo1c. CHO/IR/IRS-1 cells were transiently transfected with either EYFP (empty vector), EYFP-Myo1c WT, or K111A. Cell lysates from either basal or insulin-treated cells were subjected to immunoprecipitation with anti-GFP antibody. The ATPase activities were measured as described in Figure 5A. Immunoprecipitates were analyzed by western blot with the use of anti-GFP antibody. The experiment was performed three times, and the images are from a representative experiment.

137 mM NaCl, 10% glycerol, 25 mM Tris, pH 7.4) supplemented with Complete protease inhibitor mixture (Roche) and phosphatase inhibitors (2 mM sodium orthovanadate, 1 mM pyrophosphate, 10 mM sodium fluoride) at 4°C. For Myo1c/calmodulin interaction studies, the cells were lysed in lysis buffer containing 1 μM $CaCl_2$ supplemented with EDTA-free Complete protease inhibitor mixture (Roche) and phosphatase inhibitors. For BAPTA-AM treatment, the cells were incubated with BAPTA-AM followed by insulin in a modified Krebs-Ringer Phosphate buffer in which 1 mM $CaCl_2$ was replaced by 5 mM EGTA (120 mM NaCl, 600 μM Na_2HPO_4, 400 μM NaH_2PO_4, 6 mM KCl, 1.2 mM $MgSO_4$, 5 mM EGTA, 12.5 mM HEPES, pH 7.4) and lysed in lysis buffer supplemented with 1 mM EGTA, protease, and phosphatase inhibitors. 3T3-L1 adipocyte fractionation was carried out as described previously (Larance et al., 2005). Pulldown or immunoprecipitation was performed with 14-3-3-coupled sepharose, glutathione sepharose, or specific antibodies (anti-GFP, anti-GST, anti-Myo1c, and anti-CaMKII) coupled to protein G sepharose (Pierce; Rockford, IL). Beads were washed with lysis buffer and PBS and boiled in sample buffer. SDS-PAGE and western blotting was performed according to standard protocols. The 14-3-3 overlay assay was carried out as follows. Subsequent to SDS-PAGE, proteins were transferred to PVDF membrane. For phosphatase treatment of blot prior to overlay, the blot was incubated with alkaline phosphatase buffer (200 mM Tris, pH 8.0, 100 mM $MgCl_2$) containing 100 U/ml of shrimp alkaline phosphatase (Roche) at 37°C overnight. After incubating the membrane in blocking solution (2% (w/v) BSA in TBS/Tween 20 (0.1%, v/v)), the membrane was incubated with either GST protein or GST-14-3-3 fusion protein in blocking solution for 1 hr, followed by primary (anti-GST) and secondary antibody incubations.

Phosphorylation In Vivo and In Vitro

For in vivo γ^{32}P labeling, 3T3-L1 adipocytes were incubated in serum-free and phosphate-free DMEM for 1 hr followed by serum-free DMEM containing 2.7 mCi [^{32}P]orthophosphate per 10 cm dish for 3 hr prior to insulin stimulation. In vitro CaMKII phosphorylation assay was performed as described (Konstantopoulos et al., 2007) with modifications. To activate GST-CaMKIIα fusion protein (Cell Signaling Technology), the kinase was preincubated in kinase buffer (50 mM Tris, pH 7.5, 10 mM $MgCl_2$, 2 mM DTT, 0.1 mM EDTA, 2 mM $CaCl_2$, 100 μM ATP, 1.2 μM calmodulin [Sigma]) for 10 min at 30°C. Inactive GST-CaMKIIα, which was preincubated in kinase buffer in the absence of $CaCl_2$ and calmodulin, was used as control. Immunoprecipitated Myo1c was incubated with kinase buffer only, active GST-CaMKIIα or inactive GST-CaMKIIα for 5 min at 30°C. For in vitro ^{32}P labeling of EYFP-Myo1c, 3 μCi [γ^{32}P]ATP was added to each sample prior to CaMKII phosphorylation. The reaction was stopped by boiling in sample buffer. The phosphorylation of Myo1c and EYFP-Myo1c was analyzed by 14-3-3 overlay assay and autoradiography, respectively. For measuring CaMKII kinase activity in 3T3-L1 adipocyte lysates, the assay was carried out directly on the agarose beads bound with immunoprecipitated CaMKII using SignaTECT CaMK Assay System (Promega) according to the manufacturer's protocol. The ^{32}P labeling of the peptide substrate was analyzed by scintillation counting.

In Vitro ATPase Assay

For assay of EYFP-Myo1c immunoprecipitated from CHO/IR/IRS-1 cells, the Myo1c-bound beads were washed three times with ATPase reaction buffer (30 mM Tris, pH 7.5, 20 mM KCl, 1 mM $MgCl_2$, 1 μM $CaCl_2$), and the ATPase reactions were carried out directly on the beads in the ATPase reaction buffer containing 100 μM actin, 500 μM ATP, and 2 μCi[γ^{32}P]ATP at 37°C. For ATPase assay after in vitro CaMKII phosphorylation of Myo1c, the CaMKII was removed and the beads were washed three times with ATPase reaction buffer. The beads were incubated with either 46 ng GST or 100 ng GST-14-3-3 for 30 min. The beads were washed, and the ATPase reactions were carried out in the presence of 1 μM tat-CN21. The reactions were stopped by placing on ice. Three microliters of each reaction were spotted onto polyethyleneimine cellulose TLC plate, and the inorganic phosphate was separated as described (Bultman et al., 2005). The amounts of [γ^{32}P]Pi and [γ^{32}P]ATP were measured by autoradiography and quantified by densitometry.

Mass Spectrometry Analysis

Mass spectrometry identification of 14-3-3-binding proteins was performed as described previously (Ramm et al., 2006).

Immunoflorescence Analysis

Immunoflorescence staining of HA-GLUT4-expressing 3T3-L1 adipocytes was performed as previously described (Ramm et al., 2006). Images were obtained using the Leica TCS SP2 confocal laser scanning microscope. A region of interest (ROI) was set around each cell, and the amount of fluorescence per unit area was quantified using ImageJ software (National Institutes of Health).

2-Deoxyglucose Uptake

3T3-L1 adipocytes were preincubated with either DMSO for 45 min, 10 μM KN-62 for 45 min, 5 μM tat-CN21 for 30 min, or 5 μM tat-ctrl for 30 min in KRP buffer (120 mM NaCl, 600 μM Na_2HPO_4, 400 μM NaH_2PO_4, 6 mM KCl, 1.2 mM $MgSO_4$, 1 mM $CaCl_2$, 12.5 mM HEPES, pH 7.4) prior to 100 nM insulin stimulation for another 15 min. Uptake of 2DOG (Sigma) and ^{3}H-2DOG (Perkin Elmer Life Science; Melbourne, Australia) was measured over the final 5 min of insulin stimulation and analyzed by scintillation counting.

Statistical Analysis

Results are given as mean ± SEM. Statistical analyses were performed by using a Student's t test and $p < 0.05$ was taken to indicate a significant difference.

SUPPLEMENTAL DATA

Supplemental Data include one figure and one table and can be found online at http://www.cell.com/cellmetabolism/supplemental/S1550-4131(08)00296-9.

ACKNOWLEDGMENTS

The authors wish to thank M. Czech, J. Hancock, W. Hunziker, U. Bayer, and P. Shepherd for the kind gift of reagents. We also thank T. Brummer and C. Schmitz-Peiffer for critical evaluation of the manuscript and John Hammer and Mike Ostap for invaluable discussion.

This work was supported by grants from the National Health and Medical Research Council of Australia and Diabetes Australia Research Trust (to D.E.J.). The Bioanalytical Mass Spectrometry Facility, University of New South Wales (UNSW), was supported by grants from the Australian Government Systemic Infrastructure Initiative and Major National Research Facilities Program (UNSW node of the Australian Proteome Analysis Facility) and by the UNSW Capital Grants Scheme.

Received: October 20, 2007
Revised: March 2, 2008
Accepted: September 19, 2008
Published: November 4, 2008

REFERENCES

Bai, L., Wang, Y., Fan, J., Chen, Y., Ji, W., Qu, A., Xu, P., James, D.E., and Xu, T. (2007). Dissecting multiple steps of GLUT4 trafficking and identifying the sites of insulin action. Cell Metab. *5*, 47–57.

Barylko, B., Wagner, M.C., Reizes, O., and Albanesi, J.P. (1992). Purification and characterization of a mammalian myosin I. Proc. Natl. Acad. Sci. USA *89*, 490–494.

Barylko, B., Jung, G., and Albanesi, J.P. (2005). Structure, function, and regulation of myosin 1C. Acta Biochim. Pol. *52*, 373–380.

Batters, C., Wallace, M.I., Coluccio, L.M., and Molloy, J.E. (2004). A model of stereocilia adaptation based on single molecule mechanical studies of myosin I. Philos. Trans. R. Soc. Lond. B Biol. Sci. *359*, 1895–1905.

(D) Quantification of ATPase assays. The values of [γ^{32}P]Pi and [γ^{32}P]ATP were measured by densitometry. The ratio of [γ^{32}P]Pi to [γ^{32}P]ATP was calculated, and the background signal corresponding to Myo1c K111A was subtracted. The ratio corresponding to Myo1c WT immunoprecipitated from basal cells was normalized to 1 arbitrary unit. The value of each condition represents the mean ± SEM of three independent experiments. *$p < 0.05$ versus unstimulated cells.

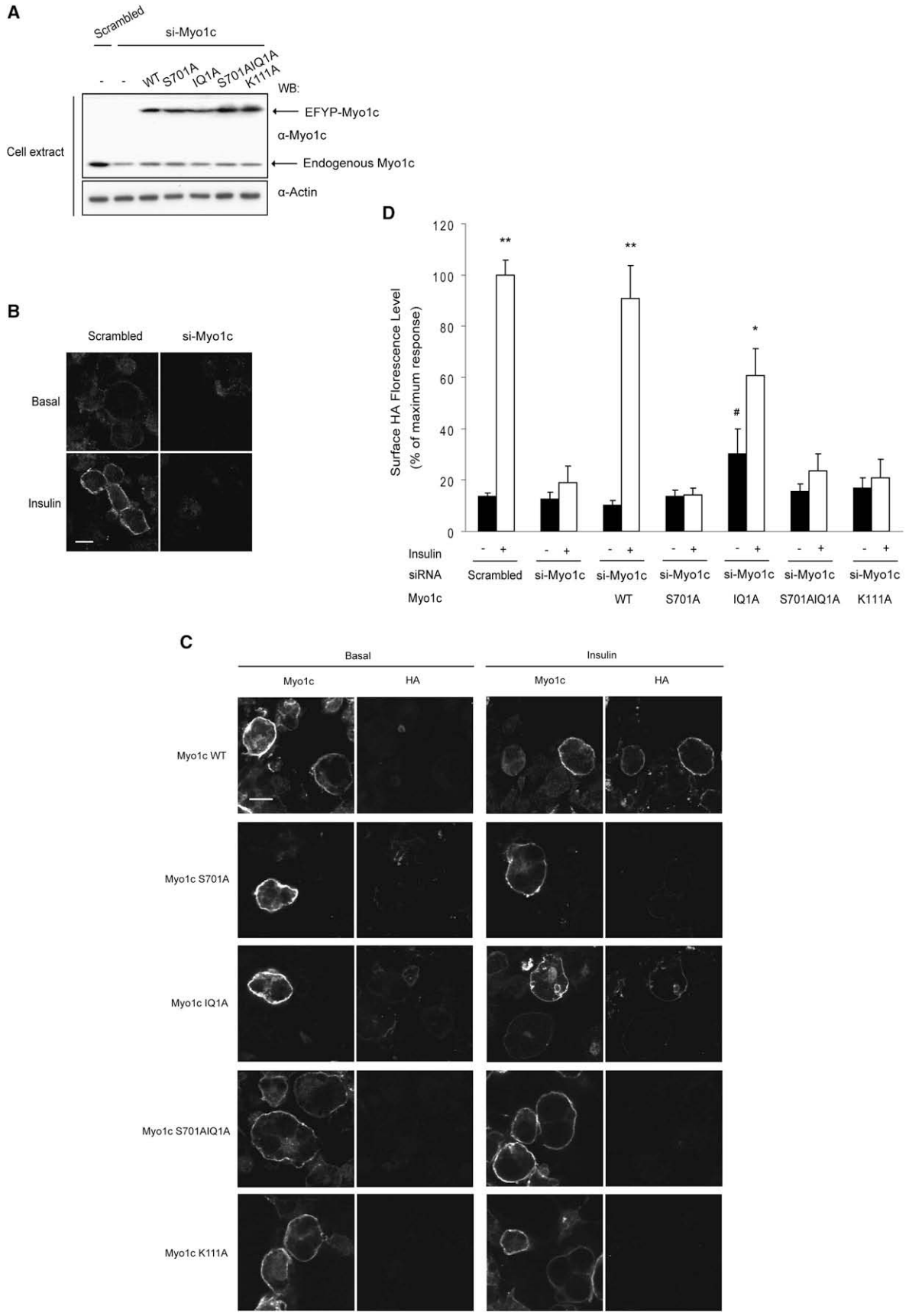
A
Scrambled
si-Myo1c
- - WT S701A IQ1A S701AIQ1A K111A
WB:
EFYP-Myo1c
α-Myo1c
Cell extract
Endogenous Myo1c
α-Actin
B
Scrambled
si-Myo1c
Basal
Insulin
D
Surface HA Florescence Level (% of maximum response)
120
100
80
60
40
20
0
**
**
*
#
Insulin
siRNA
Myo1c
Scrambled
si-Myo1c
si-Myo1c WT
si-Myo1c S701A
si-Myo1c IQ1A
si-Myo1c S701AIQ1A
si-Myo1c K111A
C
Basal
Insulin
Myo1c
HA
Myo1c WT
Myo1c S701A
Myo1c IQ1A
Myo1c S701AIQ1A
Myo1c K111A

Benzinger, A., Muster, N., Koch, H.B., Yates, J.R., 3rd, and Hermeking, H. (2005). Targeted proteomic analysis of 14–3-3 sigma, a p53 effector commonly silenced in cancer. Mol. Cell. Proteomics *4*, 785–795.

Bose, A., Guilherme, A., Robida, S.I., Nicoloro, S.M., Zhou, Q.L., Jiang, Z.Y., Pomerleau, D.P., and Czech, M.P. (2002). Glucose transporter recycling in response to insulin is facilitated by myosin Myo1c. Nature *420*, 821–824.

Bose, A., Robida, S., Furcinitti, P.S., Chawla, A., Fogarty, K., Corvera, S., and Czech, M.P. (2004). Unconventional myosin Myo1c promotes membrane fusion in a regulated exocytic pathway. Mol. Cell. Biol. *24*, 5447–5458.

Brozinick, J.T., Jr., Reynolds, T.H., Dean, D., Cartee, G., and Cushman, S.W. (1999). 1-[N, O-bis-(5-isoquinolinesulphonyl)-N-methyl-L-tyrosyl]-4- phenylpiperazine (KN-62), an inhibitor of calcium-dependent camodulin protein kinase II, inhibits both insulin- and hypoxia-stimulated glucose transport in skeletal muscle. Biochem. J. *339*, 533–540.

Bruton, J.D., Katz, A., and Westerblad, H. (1999). Insulin increases near-membrane but not global Ca2+ in isolated skeletal muscle. Proc. Natl. Acad. Sci. USA *96*, 3281–3286.

Bultman, S.J., Gebuhr, T.C., and Magnuson, T. (2005). A Brg1 mutation that uncouples ATPase activity from chromatin remodeling reveals an essential role for SWI/SNF-related complexes in beta-globin expression and erythroid development. Genes Dev. *19*, 2849–2861.

Chacko, S., Jacob, S.S., and Horiuchi, K.Y. (1994). Myosin I from mammalian smooth muscle is regulated by caldesmon-calmodulin. J. Biol. Chem. *269*, 15803–15807.

Chapman, E.R., Au, D., Alexander, K.A., Nicolson, T.A., and Storm, D.R. (1991). Characterization of the calmodulin binding domain of neuromodulin. Functional significance of serine 41 and phenylalanine 42. J. Biol. Chem. *266*, 207–213.

Colbran, R.J., Fong, Y.L., Schworer, C.M., and Soderling, T.R. (1988). Regulatory interactions of the calmodulin-binding, inhibitory, and autophosphorylation domains of Ca2+/calmodulin-dependent protein kinase II. J. Biol. Chem. *263*, 18145–18151.

Davies, K.D., Alvestad, R.M., Coultrap, S.J., and Browning, M.D. (2007). alphaCaMKII autophosphorylation levels differ depending on subcellular localization. Brain Res. *1158*, 39–49.

DeFeo-Jones, D., Barnett, S.F., Fu, S., Hancock, P.J., Haskell, K.M., Leander, K.R., McAvoy, E., Robinson, R.G., Duggan, M.E., Lindsley, C.W., et al. (2005). Tumor cell sensitization to apoptotic stimuli by selective inhibition of specific Akt/PKB family members. Mol. Cancer Ther. *4*, 271–279.

Gillespie, P.G., and Cyr, J.L. (2002). Calmodulin binding to recombinant myosin-1c and myosin-1c IQ peptides. BMC Biochem. *3*, 31.

Hokanson, D.E., Laakso, J.M., Lin, T., Sept, D., and Ostap, E.M. (2006). Myo1c binds phosphoinositides through a putative pleckstrin homology domain. Mol. Biol. Cell *17*, 4856–4865.

Houdusse, A., Gaucher, J.F., Krementsova, E., Mui, S., Trybus, K.M., and Cohen, C. (2006). Crystal structure of apo-calmodulin bound to the first two IQ motifs of myosin V reveals essential recognition features. Proc. Natl. Acad. Sci. USA *103*, 19326–19331.

Huang, J., Imamura, T., Babendure, J.L., Lu, J.C., and Olefsky, J.M. (2005). Disruption of microtubules ablates the specificity of insulin signaling to GLUT4 translocation in 3T3–L1 adipocytes. J. Biol. Chem. *280*, 42300–42306.

Huang, S., Lifshitz, L.M., Jones, C., Bellve, K.D., Standley, C., Fonseca, S., Corvera, S., Fogarty, K.E., and Czech, M.P. (2007). Insulin stimulates membrane fusion and GLUT4 accumulation in clathrin coats on adipocyte plasma membranes. Mol. Cell. Biol. *27*, 3456–3469.

Inagaki, N., Nishizawa, M., Arimura, N., Yamamoto, H., Takeuchi, Y., Miyamoto, E., Kaibuchi, K., and Inagaki, M. (2000). Activation of Ca2+/calmodulin-dependent protein kinase II within post-synaptic dendritic spines of cultured hippocampal neurons. J. Biol. Chem. *275*, 27165–27171.

Inoue, M., Chang, L., Hwang, J., Chiang, S.H., and Saltiel, A.R. (2003). The exocyst complex is required for targeting of Glut4 to the plasma membrane by insulin. Nature *422*, 629–633.

Ishiguro, K., Green, T., Rapley, J., Wachtel, H., Giallourakis, C., Landry, A., Cao, Z., Lu, N., Takafumi, A., Goto, H., et al. (2006). Ca2+/calmodulin-dependent protein kinase II is a modulator of CARMA1-mediated NF-kappaB activation. Mol. Cell. Biol. *26*, 5497–5508.

Jin, J., Smith, F.D., Stark, C., Wells, C.D., Fawcett, J.P., Kulkarni, S., Metalnikov, P., O'Donnell, P., Taylor, P., Taylor, L., et al. (2004). Proteomic, functional, and domain-based analysis of in vivo 14–3-3 binding proteins involved in cytoskeletal regulation and cellular organization. Curr. Biol. *14*, 1436–1450.

Kanzaki, M., and Pessin, J.E. (2001). Insulin-stimulated GLUT4 translocation in adipocytes is dependent upon cortical actin remodeling. J. Biol. Chem. *276*, 42436–42444.

Konstantopoulos, N., Marcuccio, S., Kyi, S., Stoichevska, V., Castelli, L.A., Ward, C.W., and Macaulay, S.L. (2007). A purine analog kinase inhibitor, calcium/calmodulin-dependent protein kinase II inhibitor 59, reveals a role for calcium/calmodulin-dependent protein kinase II in insulin-stimulated glucose transport. Endocrinology *148*, 374–385.

Koumanov, F., Jin, B., Yang, J., and Holman, G.D. (2005). Insulin signaling meets vesicle traffic of GLUT4 at a plasma-membrane-activated fusion step. Cell Metab. *2*, 179–189.

Larance, M., Ramm, G., Stockli, J., van Dam, E.M., Winata, S., Wasinger, V., Simpson, F., Graham, M., Junutula, J.R., Guilhaus, M., and James, D.E. (2005). Characterization of the role of the Rab GTPase-activating protein AS160 in insulin-regulated GLUT4 trafficking. J. Biol. Chem. *280*, 37803–37813.

Mackintosh, C. (2004). Dynamic interactions between 14–3-3 proteins and phosphoproteins regulate diverse cellular processes. Biochem. J. *381*, 329–342.

Martin, L.B., Shewan, A., Millar, C.A., Gould, G.W., and James, D.E. (1998). Vesicle-associated membrane protein 2 plays a specific role in the insulin-dependent trafficking of the facilitative glucose transporter GLUT4 in 3T3–L1 adipocytes. J. Biol. Chem. *273*, 1444–1452.

Meek, S.E., Lane, W.S., and Piwnica-Worms, H. (2004). Comprehensive proteomic analysis of interphase and mitotic 14–3-3-binding proteins. J. Biol. Chem. *279*, 32046–32054.

Millar, C.A., Powell, K.A., Hickson, G.R., Bader, M.F., and Gould, G.W. (1999). Evidence for a role for ADP-ribosylation factor 6 in insulin-stimulated glucose

Figure 6. S701 Phosphorylation and ATPase Activity of Myo1c Are Necessary for Insulin-Regulated GLUT4 Translocation

(A) Amounts of different EYFP-Myo1c proteins and endogenous Myo1c protein in HA-GLUT4-expressing 3T3-L1 adipocytes after coexpression of Myo1c-targeted siRNA (si-Myo1c) and EYFP-Myo1c for 72 hr were revealed by western blot with the use of anti-Myo1c and anti-Actin antibodies.

(B) Immunofluorescence analysis of surface HA in scrambled and Myo1c knockdown HA-GLUT4-expressing 3T3-L1 adipocytes. Basal or insulin-treated cells were fixed and stained for surface HA with anti-HA antibody (red). The scale bar represents 15 μm.

(C) Immunofluorescence analysis of surface HA in Myo1c-re-expressing cells. HA-GLUT4-expressing 3T3-L1 adipocytes were coelectroporated with si-Myo1c and EYFP-Myo1c WT, S701A, IQ1A, S701AIQ1A double mutant, or K111A. After 72 hr, basal and insulin-treated cells were fixed and stained for surface HA with anti-HA antibody (red). After permeabilization with 0.1% saponin, EYFP-Myo1c was stained with anti-GFP antibody (green). Two cells are shown in each condition. The scale bar represents 15 μm.

(D) The average surface HA fluorescence level (Cy3) of each condition is shown as percentage of maximum response of insulin-treated cells expressing scrambled siRNA and represents the mean ± SEM of three independent experiments, within which 15 cells were assayed in each experiment. #$p < 0.05$ versus unstimulated cells expressing si-Myo1c/Myo1c WT; *$p < 0.05$, **$p < 0.005$ versus unstimulated cells.

transporter-4 (GLUT4) trafficking in 3T3–L1 adipocytes. J. Biol. Chem. *274*, 17619–17625.

Olson, A.L., Trumbly, A.R., and Gibson, G.V. (2001). Insulin-mediated GLUT4 translocation is dependent on the microtubule network. J. Biol. Chem. *276*, 10706–10714.

Phillips, K.R., Tong, S., Goodyear, R., Richardson, G.P., and Cyr, J.L. (2006). Stereociliary myosin-1c receptors are sensitive to calcium chelation and absent from cadherin 23 mutant mice. J. Neurosci. *26*, 10777–10788.

Ramm, G., Larance, M., Guilhaus, M., and James, D.E. (2006). A role for 14–3-3 in insulin-stimulated GLUT4 translocation through its interaction with the RabGAP AS160. J. Biol. Chem. *281*, 29174–29180.

Reizes, O., Barylko, B., Li, C., Sudhof, T.C., and Albanesi, J.P. (1994). Domain structure of a mammalian myosin I beta. Proc. Natl. Acad. Sci. USA *91*, 6349–6353.

Rubio, M.P., Geraghty, K.M., Wong, B.H., Wood, N.T., Campbell, D.G., Morrice, N., and Mackintosh, C. (2004). 14–3-3-affinity purification of over 200 human phosphoproteins reveals new links to regulation of cellular metabolism, proliferation and trafficking. Biochem. J. *379*, 395–408.

Sano, H., Kane, S., Sano, E., Miinea, C.P., Asara, J.M., Lane, W.S., Garner, C.W., and Lienhard, G.E. (2003). Insulin-stimulated phosphorylation of a Rab GTPase-activating protein regulates GLUT4 translocation. J. Biol. Chem. *278*, 14599–14602.

Stauffer, E.A., Scarborough, J.D., Hirono, M., Miller, E.D., Shah, K., Mercer, J.A., Holt, J.R., and Gillespie, P.G. (2005). Fast adaptation in vestibular hair cells requires Myosin-1c activity. Neuron *47*, 541–553.

Tang, N., Lin, T., and Ostap, E.M. (2002). Dynamics of myo1c (myosin-ibeta) lipid binding and dissociation. J. Biol. Chem. *277*, 42763–42768.

Tokumitsu, H., Chijiwa, T., Hagiwara, M., Mizutani, A., Terasawa, M., and Hidaka, H. (1990). KN-62, 1-[N,O-bis(5-isoquinolinesulfonyl)-N-methyl-L-tyrosyl]-4-phenylpiperazi ne, a specific inhibitor of Ca2+/calmodulin-dependent protein kinase II. J. Biol. Chem. *265*, 4315–4320.

Tong, P., Khayat, Z.A., Huang, C., Patel, N., Ueyama, A., and Klip, A. (2001). Insulin-induced cortical actin remodeling promotes GLUT4 insertion at muscle cell membrane ruffles. J. Clin. Invest. *108*, 371–381.

Tsui, J., Inagaki, M., and Schulman, H. (2005). Calcium/calmodulin-dependent protein kinase II (CaMKII) localization acts in concert with substrate targeting to create spatial restriction for phosphorylation. J. Biol. Chem. *280*, 9210–9216.

Vest, R.S., Davies, K.D., O'Leary, H., Port, J.D., and Bayer, K.U. (2007). Dual mechanism of a natural CaMKII inhibitor. Mol. Biol. Cell *18*, 5024–5033.

Wagner, M.C., Barylko, B., and Albanesi, J.P. (1992). Tissue distribution and subcellular localization of mammalian myosin I. J. Cell Biol. *119*, 163–170.

Wagner, M.C., Blazer-Yost, B.L., Boyd-White, J., Srirangam, A., Pennington, J., and Bennett, S. (2005). Expression of the unconventional myosin Myo1c alters sodium transport in M1 collecting duct cells. Am. J. Physiol. Cell Physiol. *289*, C120–C129.

Wang, F.S., Liu, C.W., Diefenbach, T.J., and Jay, D.G. (2003). Modeling the role of myosin 1c in neuronal growth cone turning. Biophys. J. *85*, 3319–3328.

Watanabe, M., Nomura, K., Ohyama, A., Ishikawa, R., Komiya, Y., Hosaka, K., Yamauchi, E., Taniguchi, H., Sasakawa, N., Kumakura, K., et al. (2005). Myosin-Va Regulates Exocytosis through the Submicromolar Ca2+-dependent Binding of Syntaxin-1A. Mol. Biol. Cell *16*, 4519–4530.

Whitehead, J.P., Molero, J.C., Clark, S., Martin, S., Meneilly, G., and James, D.E. (2001). The role of Ca2+ in insulin-stimulated glucose transport in 3T3–L1 cells. J. Biol. Chem. *276*, 27816–27824.

Wilker, E., and Yaffe, M.B. (2004). 14–3-3 Proteins–a focus on cancer and human disease. J. Mol. Cell. Cardiol. *37*, 633–642.

Wright, D.C., Fick, C.A., Olesen, J.B., Lim, K., Barnes, B.R., and Craig, B.W. (2004). A role for calcium/calmodulin kinase in insulin stimulated glucose transport. Life Sci. *74*, 815–825.

Yaffe, M.B., Rittinger, K., Volinia, S., Caron, P.R., Aitken, A., Leffers, H., Gamblin, S.J., Smerdon, S.J., and Cantley, L.C. (1997). The structural basis for 14–3-3:phosphopeptide binding specificity. Cell *91*, 961–971.

Yang, C., Coker, K.J., Kim, J.K., Mora, S., Thurmond, D.C., Davis, A.C., Yang, B., Williamson, R.A., Shulman, G.I., and Pessin, J.E. (2001). Syntaxin 4 heterozygous knockout mice develop muscle insulin resistance. J. Clin. Invest. *107*, 1311–1318.

Yu, C., Cresswell, J., Loffler, M.G., and Bogan, J.S. (2007). The glucose transporter 4-regulating protein TUG is essential for highly insulin-responsive glucose uptake in 3T3–L1 adipocytes. J. Biol. Chem. *282*, 7710–7722.

Zhu, T., Sata, M., and Ikebe, M. (1996). Functional expression of mammalian myosin I beta: analysis of its motor activity. Biochemistry *35*, 513–522.

Zhu, T., Beckingham, K., and Ikebe, M. (1998). High affinity Ca2+ binding sites of calmodulin are critical for the regulation of myosin Ibeta motor function. J. Biol. Chem. *273*, 20481–20486.